Channels 8:5, 458–466; September/October 2014; © 2014 Taylor & Francis Group, LLC

Mitochondria represent another locale for the divalent metal transporter 1 (DMT1)

Natascha A Wolff[1,*], Laura M Garrick[2], Lin Zhao[2], Michael D Garrick[2], and Frank Thévenod[1,*]

[1]Institute of Physiology; Pathophysiology & Toxicology; University of Witten/Herdecke; Witten, Germany; [2]Department of Biochemistry; State University of New York; Buffalo, NY USA

The divalent metal transporter (DMT1) is well known for its roles in duodenal iron absorption across the apical enterocyte membrane, in iron efflux from the endosome during transferrin-dependent cellular iron acquisition, as well as in uptake of non-transferrin bound iron in many cells. Recently, using multiple approaches, we have obtained evidence that the mitochondrial outer membrane is another subcellular locale of DMT1 expression. While iron is of vital importance for mitochondrial energy metabolism, its delivery is likely to be tightly controlled due to iron's damaging redox properties. Here we provide additional support for a role of DMT1 in mitochondrial iron acquisition by immunofluorescence colocalization with mitochondrial markers in cells and isolated mitochondria, as well as flow cytometric quantification of DMT1-positive mitochondria from an inducible expression system. Physiological consequences of mitochondrial DMT1 expression are discussed also in consideration of other DMT1 substrates, such as manganese, relevant to mitochondrial antioxidant defense.

Keywords: divalent metal transporter 1 (DMT1), flow cytometry, immunofluorescence microscopy, iron transport, mitochondrial outer membrane

Abbreviations: AIF, apoptosis-inducing factor; BSA, bovine serum albumin; CHO, Chinese hamster ovary; COXII, cytochrome C oxidase subunit II; DMT1, divalent metal transporter 1; HEK293, human embryonic kidney cells; IRE, iron responsive element; Lamp1, lysosome-associated membrane protein 1; MRB, Mitochondrial Resuspending Buffer; OMM, outer mitochondrial membrane; PBS, phosphate-buffered saline; Tom6/Tom20, translocase of the outer mitochondrial membrane 6 kDa subunit homolog/20 kDa subunit, respectively; Tf, transferrin; VDAC1, voltage-dependent anion-selective channel protein 1

*Correspondence to: Frank Thévenod; Email: frank.thevenod@uni-wh.de; Natascha A Wolff; Email: natascha.wolff@uni-wh.de

Submitted: 07/13/2014

Revised: 08/12/2014

Accepted: 08/15/2014

http://dx.doi.org/10.4161/19336950.2014.956564

Addendum to: Wolff NA, Ghio AJ, Garrick LM, Garrick MD, Zhao L, Fenton RA, Thévenod F. Evidence for mitochondrial localization of divalent metal transporter 1 (DMT1). FASEB J 2014; 28:2134-45; http://dx.doi.org/10.1096/fj.13-24056

Introduction

Iron is an essential metal that is required for erythropoiesis and a key component of mitochondrial enzymes in all cells and is therefore indispensable for cellular survival. The vital importance of iron for life is due to its redox properties: In biological systems iron exists as the ferrous (2+) and ferric (3+) forms. Yet the same properties are responsible for iron being a Fenton reagent that is involved in the creation of toxic free radicals making handling of iron metabolism a key issue for cells. The majority of cellular iron enters mitochondria for heme and iron-sulfur cluster synthesis.[1-3] Because of the importance of iron in oxidative metabolism, it would be expected that import of iron–as well as of the redox active essential metals manganese and copper–into mitochondria should be carefully controlled by specific influx transporters. Indeed, iron flux through the inner mitochondrial membrane is regulated through differential turnover of mitoferrins.[4] In contrast, until recently it has been assumed (despite the absence of any experimental evidence) that transport of essential metal ions, including iron, across the outer mitochondrial membrane should occur via free permeation of these metal ions through voltage-dependent anion-selective channels (VDACs),[5] with the naïve notion that VDACs are large nonselective diffusion pores through which small hydrophilic solutes can freely diffuse (however see Colombini).[6]

The divalent metal transporter 1 (DMT1) is well established as a participant in iron influx into the duodenum, as the major contributor to iron efflux from the endosome during the transferrin (Tf) cycle and in handling some Tf-independent entry of iron and other metals (including copper and manganese) into many cell types.[1,2,7,8] Recently, we have reported[9] multiple lines of evidence for the presence of DMT1 in the outer mitochondrial membrane (OMM) in several cell lines and tissues from multiple origins. Experimental support came from yeast-2-hybrid, co-immunoprecipitation and immunoblotting

data plus immunofluorescence microscopy of mitochondria isolated by several procedures and electron microscopy of kidney tissue. Our data suggested that any of the 4 major DMT1 isoforms' N- and C-termini localize in the OMM.

We now present additional support of DMT1's OMM presence from immunofluorescence analysis of DMT1 localizing with mitochondrial markers, flow cytometry and immunostaining of isolated mitochondria. DMT1 must be oriented on the OMM similarly to on the plasma membrane to serve as gateway for mitochondrial metal import. Preliminary evidence supports this orientation and this role. Hence, the data strongly suggest that DMT1 also plays a role in mitochondrial import of iron and other transition metals, such as manganese and copper, for storage and mitochondrial utilization.

Results

Overexpressed as well as endogenous DMT1 in CHO cells partially colocalizes with mitochondrial markers

Using a number of different approaches, we previously obtained evidence that the divalent metal transporter DMT1 is in part localized to mitochondria.[9] When rat or mouse DMT1 was overexpressed in HEK293 cells under the control of a Tet-on promoter, doxycycline induction resulted in an increase of DMT1 not only in whole cell homogenates, but also in the mitochondrial fraction, as determined by immunoblotting. Moreover, DMT1 immunostaining of mitochondria isolated from these cells also increased. We therefore assayed for colocalization of DMT1, endogenous or overexpressed, with mitochondrial markers in cultured cells. In CHO cells, there was partial, yet substantial, overlap with the mitochondrial marker VDAC1, the voltage-dependent anion channel 1 (**Fig. 1**, *arrows*). When FLAG-tagged human DMT1–1A was overexpressed in CHO cells, a punctate intracellular pattern was observed (**Fig. 2**). While the distribution was frequently distinct from that of the outer mitochondrial membrane protein Tom6 as one would expect for DMT1's endosomal/lysosomal localization, the merged images indicated colocalization in a number of spots, albeit even more was observed for endogenous DMT1 with mitochondria (**Fig. 1**). Partial co-staining was further supported by the multiplied binary images (**Fig. 2**, bottom left panel), as well as the intensity line profile (**Fig. 2**, bottom right panel); these manipulations are among those recommended to detect real, but partial colocalization.[10] The VDAC1 and Tom6 antibodies have been validated for use in CHO cells (**Fig. S1**). VDAC1 labeling overlapped completely with that for the mitochondrial apoptosis-inducing factor (AIF) (**Fig. S1**, upper panels), and staining for Tom6 largely colocalized with AIF-positive structures (**Fig. S1**, lower panels).

Detection of DMT1 in mitochondria of stably transfected HEK293 cells by flow cytometry

Because immunofluorescence data in HEK293 or CHO cells with endogenous or overexpressed DMT1 (**Figs. 1** and **2**; see also ref.[9]) relied on detecting mitochondria where their size nears the limits of fluorescence microscopy, we also tried to assess the mitochondria by flow cytometry, again extending the technical limits of the detection method. **Figure 3** displays results for uninduced HEK293 cells and HEK293 cells where DMT1 has been induced by 25 nM doxycycline with panels A-E exhibiting results for rat 1A/+IRE DMT1 while panels G-K display similar results for mouse 1B/-IRE DMT1 under the same set of conditions. Note that the levels of fluorescence for panel D and J are clearly left shifted (lower) than for E and K, respectively, reflecting increased DMT1 expression in E and K. Nearly 2/3 of events in panel C and I stain for translocase of the outer mitochondrial membrane 20-kDa subunit (Tom20) indicating that mitochondria represent that fraction of particles detected. The fractions of events in panel E and K that have a DMT1-specific signal are slightly higher. It is attractive to infer that the same population is being detected by both signals. Even if that should not be the case, the fraction is so high in both cases that one must infer that a substantial proportion of events representing mitochondria also are positive for DMT1, confirming and extending the results for immunofluorescence microscopy on isolated mitochondria. Contamination with endosomes as represented by fluorescence detected with an antibody to early endosomal antigen 1 is minimal (not shown).

Immunolocalization of DMT1 in mitochondria isolated from a rat renal proximal tubule cell line

Mitochondrial DMT1 localization had previously also been detected in rat renal cortex cryosections by immunogold electron microscopy.[9] Consistent with these findings, DMT1 immunofluorescence was detected in mitochondria isolated from a rat renal proximal tubule cell line (WKPT-0293 Cl.2),[11] with the identity of the mitochondria confirmed by fluorescence overlap with MitoTracker® as well as VDAC1 staining (**Fig. 4**).

Discussion

Mitochondria from HEK293 cells overexpressing rat or mouse DMT1 under the control of a Tet-on promoter were previously found to be positive for DMT1 in a tetracycline-dependent manner, as determined by immunoblotting.[9] Moreover, in rat renal proximal tubules, known to express DMT1 in late endosomes and lysosomes,[12] DMT1 was also detected in mitochondria by cryo-immunogold electron microscopy.[9] In order to consolidate these findings, we have presented here additional lines of evidence that DMT1 is expressed in the outer membrane of mitochondria.

Firstly, we assayed for mitochondrial localization of both heterologously expressed as well as endogenous DMT1 in the CHO cell line by confocal laser scanning fluorescence microscopy. The overexpressed human 1A/+IRE DMT1 isoform partially colocalized with the endogenous mitochondrial marker Tom6 (**Fig. 2**). Yet, more pronounced colocalization with a mitochondrial marker (VDAC1) was detected for the endogenous DMT1 in CHO cells (**Fig. 1**). Considering that DMT1 is also expressed in other

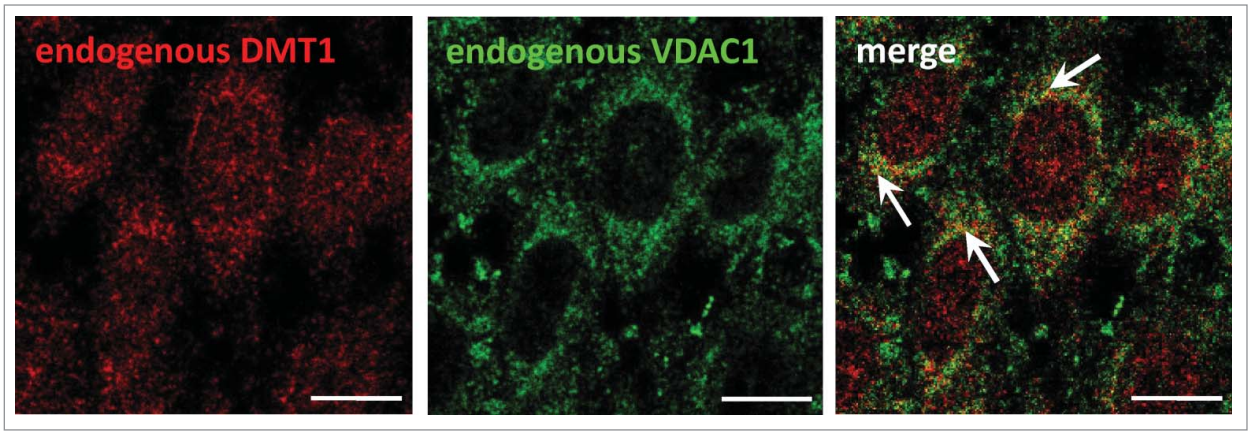

Figure 1. Localization of endogenous DMT1 partially overlaps with the mitochondrial marker VDAC1 in CHO cells. CHO cells plated at 4.5 × 10^4/cm^2 were grown for 2 d. They were then fixed, permeabilized, blocked, and subsequently stained with primary rabbit anti-rat-DMT1 (#1092–3; 2.5 μg/ml) (red) and goat anti-VDAC1 (1:25) (green) antibodies, followed by secondary Cy3-anti-rabbit and Alexa488-anti-goat antibodies. The specimens were imaged by confocal microscopy and the images analyzed as described in Materials and Methods. Arrows in the merged image point to areas of colocalization of endogenous DMT1 with endogenous VDAC1. Scale bars: 10 μm.

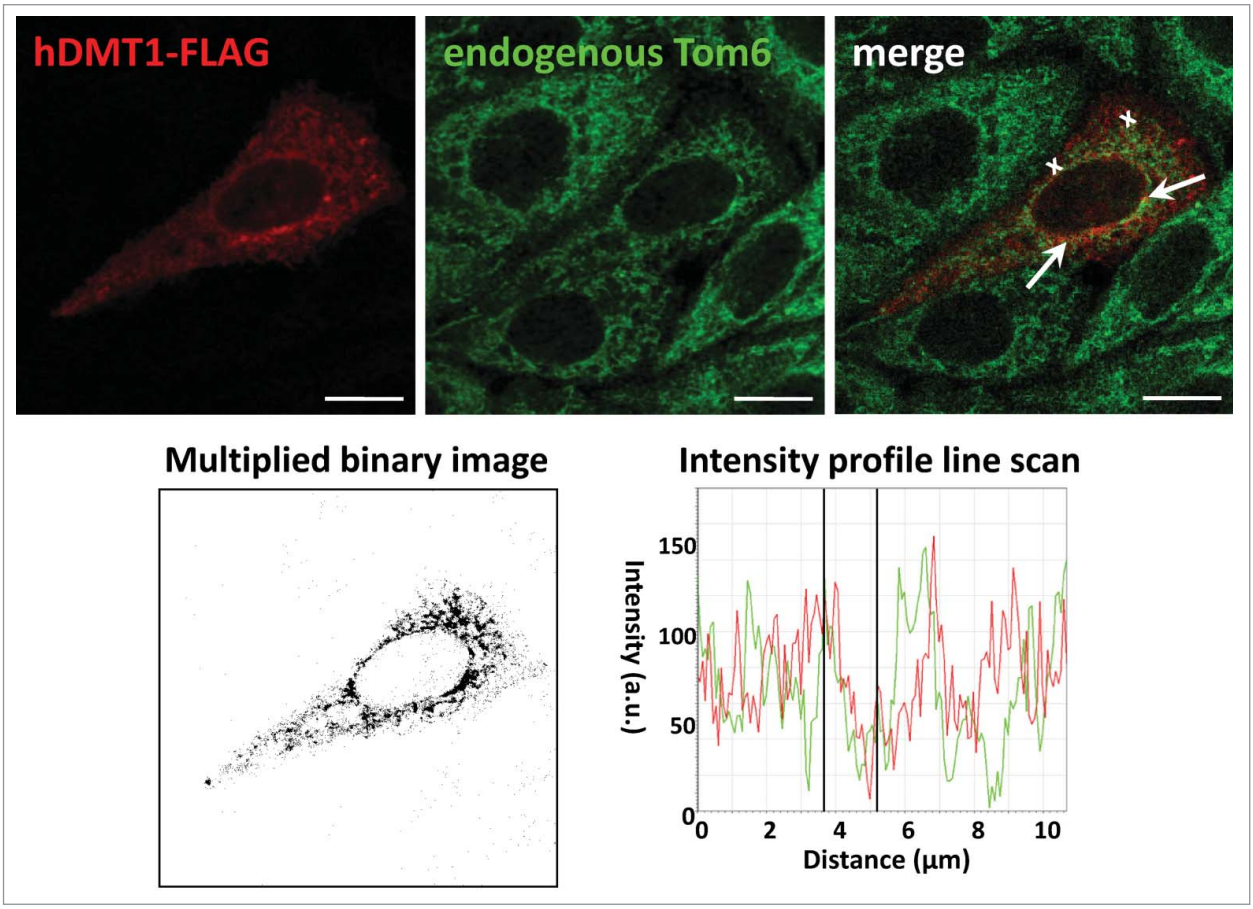

Figure 2. Transfected hDMT1–1A/+IRE partially colocalizes with endogenous Tom6 in CHO cells. CHO cells were seeded at 4.5 × 10^4 cells/cm^2 on glass coverslips and transiently transfected with hDMT1–1A/+IRE-FLAG 24h later. After 48 hrs of incubation post transfection, they were fixed, permeabilized, blocked, and then stained with primary mouse anti-FLAG (20 μg/ml) (red) and goat anti-Tom6 (1:25) (green) antibodies, followed by secondary Cy3-anti-mouse and Alexa488-anti-goat antibodies. Laser scanning confocal micrographs were acquired sequentially for the different fluorophores. To visualize colocalization, images were merged (top right panel). An intensity profile line scan (bottom right panel) was obtained along the distance indicated by the white crosses in the merged image (top right panel), and a multiplied binary image (bottom left panel) generated as detailed in *Materials and Methods*. Arrows in the merged image show areas of colocalization of transfected hDMT1–1A/IRE(+) with endogenous Tom-6. Scale bars: 10 μm.

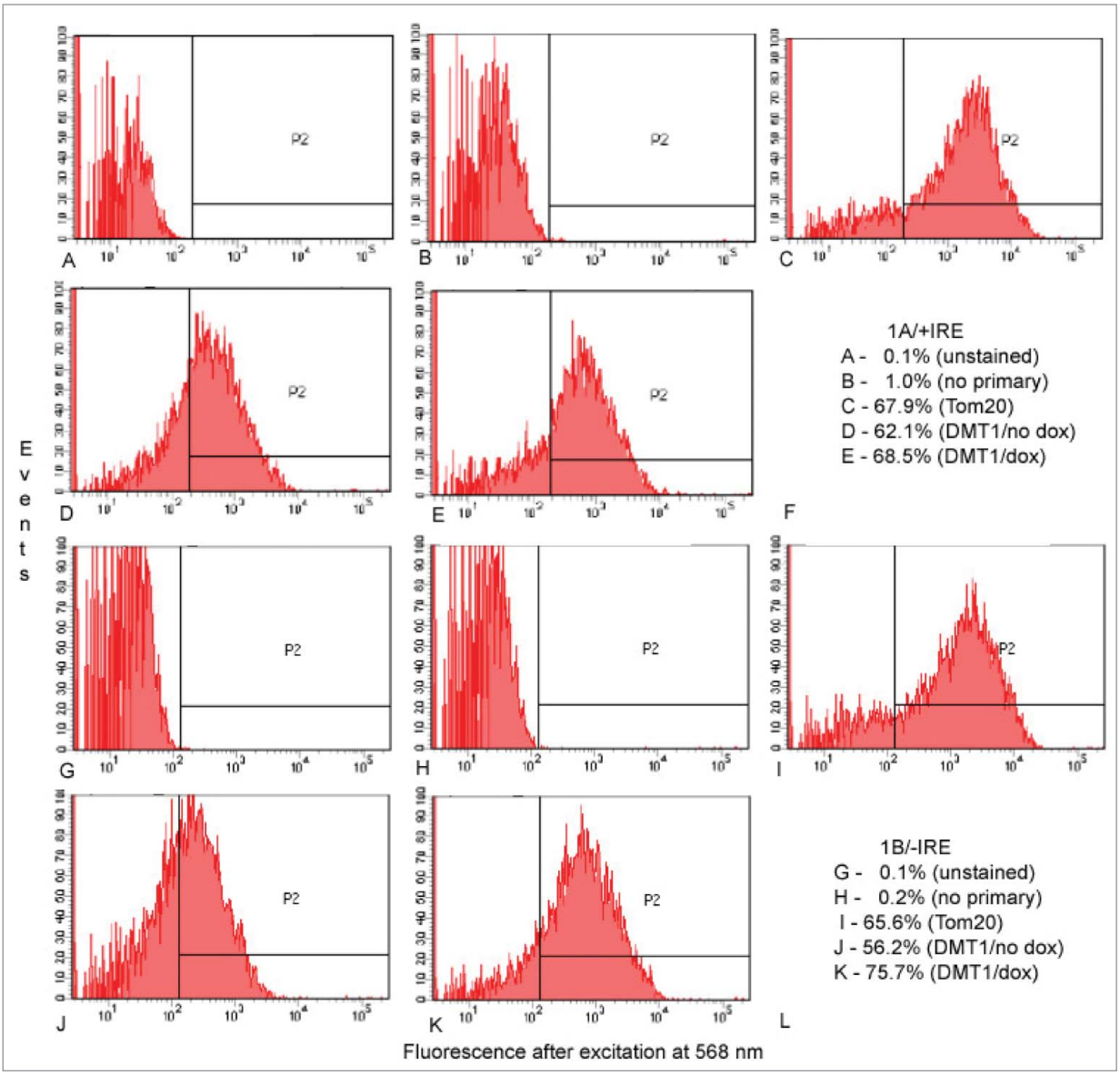

Figure 3. Detection of DMT1 in isolated mitochondria from HEK293 cells by flow cytometry. Gating on side and forward scatter excluded events smaller than expected for mitochondria as well as those so large that they might represent aggregates of mitochondria or pieces of cell membrane with (**A–E**) = 1A/+IRE DMT1 and G-K = 1B/-IRE DMT1. Then fluorescence after excitation at 568 nm was determined for (**A and G**) unstained preparations; (**B and H**) preparations stained only with secondary antibody; (**C and I**) preparations stained with anti-Tom20 then secondary antibody; (**D and J**) preparations from uninduced cells stained with 4EC DMT1 antibody then secondary antibody; (**E and K**) preparations from doxycycline-induced cells stained with 4EC DMT1 antibody then secondary antibody; (**F and L**) tabulations of the % of events in the P2 window for (**A–E**) and (**G–K**), respectively.

subcellular locations/compartments, it is not too surprising that only partial overlap with mitochondrial markers was found in untransfected cells expressing only endogenous DMT1, and even less in cells with overexpressed DMT1, where a substantial amount of the overexpressed protein is likely not to have reached its final destination. Furthermore, the use of different mitochondrial markers for colocalization of endogenous (VDAC1 in **Fig. 1**) versus overexpressed DMT1 (Tom6 in **Fig. 2**) represents an additional variable in the degree of colocalization that could contribute to an underestimation of mitochondrial localization of DMT1. We actually determined the percentage of cellular DMT1 in mitochondria of kidney cortex using subfractionation studies followed by immunoblotting (see ref. 9). Based on our calculations, we found that ~6% of total (kidney cortex homogenate) DMT1 is recovered in mitochondria whereas about 40% of total cellular DMT1 was found in the lysosomal fraction. Since it must also be assumed that DMT1 is expressed in the plasma membrane and other cellular organelles, e.g. endosomes, mitochondrial DMT1 is likely to amount to below 10% of total cellular DMT1.

During flow cytometry of mitochondria isolated from HEK293 cells

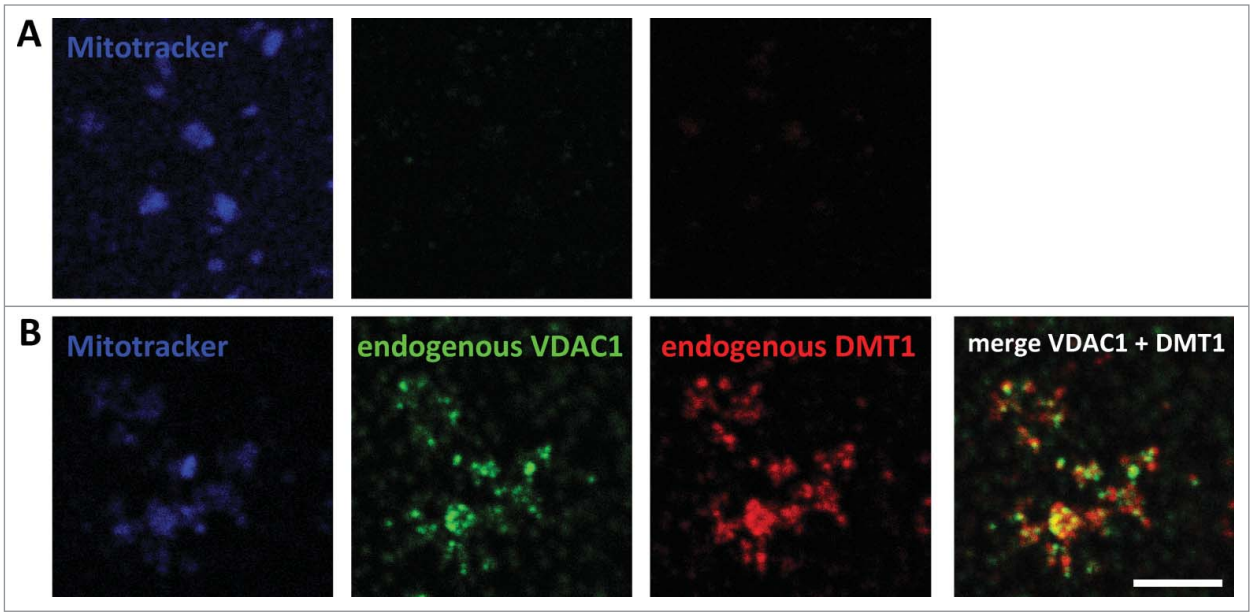

Figure 4. Immunodetection of DMT1 in mitochondria isolated from a rat renal cortical cell line. Mitochondria were isolated from WKPT-0293 Cl.2 rat renal proximal tubule cells as detailed in Materials and Methods. After loading with MitoTracker® Deep Red FM, they were left to attach to coverslips, fixed, permeabilized and blocked. They were then incubated without (**A**) or with (**B**) primary goat-anti-VDAC1 and rabbit-anti-DMT1 antibodies, followed by secondary Cy3-anti-rabbit and Alexa488-anti-goat antibodies. Confocal images were acquired and analyzed as described in Materials and Methods. Scale bar: 5 μm.

permanently transfected with mouse 1B/-IRE or rat 1A/+IRE DMT1 (**Fig. 3**) about 2/3 of events that have light scattering properties predicted for mitochondria are positive for Tom20 based on detection with a polyclonal rabbit antibody. A similar but slightly higher fraction of events is positive for DMT1. The antibody used to detect DMT1 is also a rabbit polyclonal antibody so that we could not directly assess by double label technology if the same subcellular particles have both Tom20 and DMT1. Yet the fractions with the 2 signals are so high that at least 1/3 of the events must represent the presence of both antigens.

Furthermore, percoll-purified mitochondria from the rat renal proximal tubule cell line WKPT-0293 Cl.2, previously shown to exhibit a similar subcellular DMT1 distribution as in renal proximal tubules,[12] and identified by VDAC1 and MitoTracker® staining, were also immunoreactive for DMT1 (**Fig. 4**).

What might be the functional significance of mitochondrial DMT1-mediated transport, in particular since our data indicated its localization in the OMM? As discussed previously,[9] this membrane is generally believed to be freely permeable to small molecules, including metal ions, although this assumption does not appear to be compatible with the presence of a proton gradient across the OMM.[13] Thus, other permeation pathways are likely to exist to allow for the delivery of iron and other transition metals across the OMM.[14,15] For iron, 3 transporters/channels, namely SLC22A4 (also known as OCTN1), TMEM14C and SLC25A39, a member of the mitochondrial carrier family (MCF), have been suggested to be involved,[16] based on computational screening of the mouse mitochondrial proteome database MitoCarta[17] for proteins correlated with components of the heme synthesis machinery.[18] Yet, neither SLC22A4 nor TMEM14C have otherwise been associated with divalent metal transport, and MCF proteins are considered to reside in the inner mitochondrial membrane.[19] DMT1 is well known as an Fe^{2+} carrier operating as a metal ion/proton cotransporter.[20] Yet, despite the acidic intermembrane space, we have previously suggested that in mitochondria it might nevertheless be involved in iron delivery across the OMM,[9] based on the observation that DMT1 can also mediate Fe^{2+} transport uncoupled from proton flux.[21,22] Indeed, this mode has been suggested to account for iron toxicity due to non-transferrin-bound, DMT1-mediated cell-surface iron uptake by liver[23] and heart[24] under iron overload conditions.[22] Iron may then transit through the mitochondrial chelatable iron pool,[25,26] and subsequently be stored in mitochondrial ferritin[27] or used in heme[28,29] or iron-sulfur cluster biosynthesis.[3]

Another high-affinity substrate of DMT1 is manganese.[20,21,30,31] As uncoupling from proton flux also applies to DMT1-mediated manganese transport,[21] OMM DMT1 may also be involved in manganese delivery to mitochondria. Mitochondria require manganese for protection against oxidative stress by the mitochondrial SOD2, the main antioxidant enzyme in mitochondria[32] and localized exclusively in the mitochondrial matrix,[33] and possibly non-SOD manganese antioxidants.[34] Similar to iron, manganese has been suggested to be delivered to yeast mitochondria by a kiss-and-run type mechanism of temporary contact (or fusion) with vesicles containing Smf2p,[35]

a yeast divalent metal transporter closely related to DMT1.[36] Interestingly, Smf2p has been found in the yeast mitochondrial proteome.[37] As for iron, little is known about manganese translocation across the OMM, and DMT1 is a good candidate to execute this function. Indeed, preliminary experiments on mitochondria isolated from doxycycline-induced HEK293 cells stably transfected with mDMT1–1B/-IRE or rDMT1–1A/+IRE support DMT1-mediated mitochondrial manganese uptake (data not shown). DMT1 deficiency, as resulting from certain DMT1 mutants in animals and humans, may thus also impair mitochondrial function due to compromised mitochondrial antioxidant defense. On the other hand, overexposure to manganese has been shown to result in a neurotoxic disorder with Parkinson-like symptoms, known as manganism. Manganese has been found directly to impair oxidative metabolism and interfere with mitochondrial Ca^{2+} homeostasis (for a review see ref.[38]). As DMT1 levels increase in substantia nigra cells in PD,[39] the potential DMT1-mediated transition metal overload of mitochondria in PD expected from mitochondrial DMT1 localization may thus affect mitochondrial function by mechanisms in addition to oxidative stress.

The ability of DMT1 to translocate copper is still controversial and may depend on the species and/or isoform investigated[20,30,31,40,41] or level of DMT1 expression and/or iron status.[42,43] Interaction with the copper-containing cytochrome C oxidase subunit II (COXII)[9] may suggest an involvement of DMT1 in copper delivery for metallation of this enzyme, and possibly mitochondrial SOD1, as well as to the matrix copper pool known to exist in both yeast and mammalian mitochondria.[44,45] Copper incorporation into both mitochondrial encoded COXII as well as nuclear encoded mitochondrial SOD1 have been reported to occur in the intermembrane space.[46] Yet, considering that copper for incorporation into COXII may originate from the mitochondrial matrix, rather than from the cytosol,[45] DMT1 could then only be indirectly involved in providing the metal ion for this process.

Materials and Methods

Materials

Protease inhibitor cocktail, bovine serum albumin (BSA) and paraformaldehyde were obtained from Sigma-Aldrich (Taufkirchen, Germany), poly-L-lysine from ***Santa Cruz*** Biotechnology, Inc. (Heidelberg, Germany). MitoTracker® Deep Red FM was purchased from Molecular Probes/LifeTechnologies (Darmstadt, Germany).

Antibodies

Anti-FLAG M2 mouse monoclonal antibody was from Sigma-Aldrich. Anti-AIF rabbit polyclonal antibody (H-300; sc-5586), anti-translocase of the outer mitochondrial membrane 6-kDa subunit (anti-Tom6) (goat polyclonal antibody C-14; sc-24447), and anti-VDAC1 goat polyclonal antibody (N-18; sc-8828) were obtained from Santa Cruz. A rabbit polyclonal anti-rat DMT1 directed against the peptide sequence MVLDPEEKIPDDG-ASGDHGDS,[47] representing exon 2 and part of exon 3, was generated by Immuno-Globe GmbH (Himmelstadt, Germany; designated #1092–3). This antibody detects all 4 rat DMT1 isoforms. Another antibody that detected all 4 DMT1 isoforms was directed against the putative fourth extracellular domain of the antigen[48] so it was designated 4EC. The anti-translocase of the outer mitochondrial membrane 20-kDa subunit (anti-Tom20) was purchased from Santa Cruz Biotechnology (Santa Cruz, CA; rabbit polyclonal antibody; sc-17764). Secondary Alexa-Fluor 568-conjugated goat anti-rabbit IgG was from Molecular Probes (Eugene, OR), secondary Cy3™-conjugated donkey anti-mouse and donkey anti-rabbit IgG, and Alexa Fluor® 488-conjugated donkey anti-goat IgG were obtained from Jackson ImmunoResearch Europe Ltd (Newmarket, Suffolk, UK).

hDMT1-Plasmid

The hDMT1–1A/+IRE-FLAG plasmid was a gift from Dr. Matthias Hentze, EMBL, Heidelberg, Germany. For transient expression in Chinese hamster ovary (CHO) cells, the coding sequence of hDMT1–1A/+IRE-FLAG was excised with SpeI and XhoI, and ligated into NheI/XhoI-restricted pcDNA3.1+ using the Ligate-IT Rapid Ligation Kit (USB/Affimetrix, Freiburg, Germany), after both insert and vector had been purified by agarose gel electrophoresis followed by gel elution (QIAquick Gel Extraction Kit, Qiagen, Hilden, Germany).

Methods

Transient transfection of CHO cells

CHO cells were cultured in F12 medium (Gibco) supplemented with 10% fetal bovine serum and 50 U/ml penicillin / 50 μg/ml streptomycin at 37°C and 5% CO_2. For immunofluorescence, the cells were plated on glass coverslips in 24-well plates at 4.5–5 × 10^4 cells/cm^2 in culture medium without antibiotics. After 24 h of incubation, they were transfected with FLAG-tagged hDMT1–1A/+IRE in pcDNA3.1 or empty vector using Lipofectamine2000 (Invitrogen) as per the manufacturer's instructions, with 0.8 μg plasmid and 2 μl transfection reagent per well and grown for 2 further days prior to immunofluorescence microscopy.

Culture of permanently transfected cell lines

We have previously described[9] the 2 cell lines that were permanently transfected respectively with mouse 1B/-IRE and rat 1A/+IRE DMT1 constructs in HEK293 cells. Briefly, the 2 lines were Tet-on up-regulated so that incubating them with 25 nM doxycycline led to an induction of DMT1 expression[21] This property makes the increase in DMT1 expression a hallmark for identifying DMT1.

Isolation of and flow cytometry on mitochondria from HEK293 cell lines

Mitochondrial isolation relied on a kit (89874; Thermo Scientific, Rockford, IL, USA), used according to the manufacturer's instructions where we always chose the option favoring mitochondrial purity rather than yield whenever such a choice was offered.

After isolation, mitochondria were resuspended and fixed in 2% paraformaldehyde for 10 min at room temperature, then washed twice by resuspending in PBS and centrifuging at 12000 × *g* for 5 min. After permeabilization with 0.1%

Triton X-100 for 5 min, preparations were washed twice as before with PBS, blocked with 5% bovine serum albumen in PBS and stained with primary antibody (anti-Tom20 or 4EC) overnight at 4°C, then with secondary antibody (AlexaFluor 568-conjugated goat anti-rabbit IgG) for 30 min at room temperature. After being washed 3× in PBS, the mitochondria were resuspended in 0.02% NaAzide in PBS and stored at 4°C until analysis by flow cytometry using a Becton-Dickinson (BD, San Jose, CA) Fortessa 4 laser flow cytometer with the BD FACSDiva Software package. After gating on side and forward scatter to exclude particles (events) smaller than expected for mitochondria as well as those so large that they might represent aggregates of mitochondria or pieces of cell membrane, the signal for 10,000 events was collected as designated for PE-Texas Red A which has the same spectral properties as Alexa-568.

Mitochondrial isolation from WKPT-0293 Cl.2 (in italic! FT) cells

Procedures were approved by the animal ethics committee, and animal handling was in accordance with German law on animal experimentation and the European Directive on the Protection of Animals used for Scientific Purposes (2010/63/EU). Crude mitochondria were prepared from WKPT-0293 Cl.2 cells by differential centrifugation using an adaptation of the method described by Ott.[49] Briefly, the cells were trypsinized, pelleted at 900 × g for 2 min, washed once with PBS followed by centrifugation as before, resuspended in MSH buffer (in mM: 210 mannitol, 70 sucrose, 5 Hepes, pH 7.4) with 1 mM EDTA, and then disrupted by sonication (3 × 5 0.5 sec pulses), using a Branson sonifier (Sonifier S-250D, Danbury, CT). The suspension was centrifuged (600 × g, 8 min), the supernatant recentrifuged as before, and the mitochondria pelleted from the subsequent supernatant (5,600 × g, 15 min). The mitochondrial pellet was resuspended in MRB (mitochondria resuspending buffer; in mM: 250 mannitol, 5 HEPES, pH 7.4, and 0.5 EGTA) and the mitochondria collected again by centrifugation (9,000 × g, 10 min). The crude mitochondria were further purified and recovered according to the method of Wieckowski et al.[50] In short, they were resuspended in MRB and subjected to continuous Percoll gradient centrifugation (225 mM mannitol, 25-mM HEPES, pH 7.4, 1-mM EGTA and 30% (v/v) Percoll; 95,000 × g, 30 min). The mitochondrial layer was collected, diluted with MRB, and the mitochondria pelleted (7,000 × g, 10 min). They were washed twice with Mitotracker loading buffer (in mM: 210 mannitol, 70 sucrose, 1 EDTA-Na_2, 50 Tris-HCl, pH 7.4), followed by centrifugation (7000 × g, 10 min), and the final pellet resuspended in mitotracker loading buffer.

Immunofluorescence microscopy

Non-transfected cells were plated at 4.5–6 cells × 10^4 cells/cm^2 in medium with antibiotics and stained 2 d later; transfected cells were prepared as described above. Cells were then processed and images acquired essentially as previously described.[51,52] In brief, cells were washed 2–3 times with calcium- and magnesium-containing PBS, fixed with 4% paraformaldehyde, permeabilized with 1% SDS, and blocked with 1% BSA (all in PBS at room temperature). They were then incubated with primary antibody, diluted in PBS/1% BSA as detailed in the figure legends, either overnight at 4°C or for 2 h at room temperature, followed by incubation with Cy3™- or Alexa Fluor® 488-conjugated secondary antibody (dilution 1:500–1:600) for 1 h at room temperature. The nuclei were counterstained with 0.8 mg/ml 2′-(4-ethoxyphenyl)-5-(4-methyl-L-piperazinyl)-2,5′-bi-1H-benzimidazole, 3HCl (H-33342) (Calbiochem, San Diego, CA) for 5 min, and the coverslips mounted with DAKO fluorescence mounting medium (Dako, Hamburg, Germany).

For conventional fluorescence microscopy, a Zeiss Axiovert 200 M microscope (Carl Zeiss, Jena, Germany), equipped with a Fluar 40×/ 1.3 oil immersion objective and filters for Cy3 (red), FITC (green), and 4′,6-diamidino-2-phenylindole (blue) with excitation/emission wavelengths of 545/610, 480/535, and 360/460 nm, respectively, were used. Images were analyzed with the MetaMorph software (Universal Imaging; Downingtown, PA). Confocal images were acquired using a TCS SP5 confocal laser scanning microscope (Leica, Wetzlar, Germany) with a Plan-Apochromat 63×/1.4 N.A. oil immersion objective (Leica, Wetzlar, Germany) and equipped with an argon (488 nm) and a HeNe laser (543nm) as described previously.[51] To avoid bleed-through, the specimens were scanned sequentially. Confocal images from different channels were analyzed as previously described,[52] using the LAS AF software for background subtraction and merging of images from different channels, as well as for intensity profile line scans, and ImageJ for binary pixel multiplication. These manipulations help to identify partial, but valid colocalization.[10]

Immunostaining of isolated mitochondria

Staining of mitochondria isolated from WKPT-0293 Cl.2 cells was adapted from Singh et al.[53] In brief, mitochondria isolated as described above were loaded with 500 nM MitoTracker® Deep Red FM (1 h, 4°C, with rotation at 30 rpm). They were then plated onto acid-washed (1N HCl, 50–60°C, 8–16 h), 0.1% poly-L-lysine- (Santa Cruz) coated (2 h, RT), H_2O-washed and dried coverslips, and left to attach for 1 h at 4°C. After one wash with PBS, they were fixed with 4% (w/v) paraformaldehyde in PBS (10 min, RT), permeabilized with 0.5% (v/v) Triton X-100 (10 min, RT), and blocked with 1% BSA in PBS (30 min, RT). Mitochondria were then labeled with primary antibodies (in PBS/1% BSA, ON, 4°C), followed by secondary antibodies (dilution 1:500–1:600 in PBS/1% BSA, 1 h at RT), washed, and mounted. Confocal images were acquired and analyzed as described above.

Disclosure of Potential Conflicts of Interest

No potential conflicts of interest were disclosed.

Acknowledgments

The hDMT1–1A/+IRE plasmids were provided by Dr. Matthias Hentze (EMBL, Heidelberg, Germany). Access to the BD Fortessa 4 laser flow cytometer

was provided by the State University of New York (SUNY) Buffalo Flow Cytometry Facility.

Funding

Financial support was obtained by DFG TH345/11–1, ZBAF, and the Laura and Michael Garrick Fund.

References

1. Chen C, Paw BH. Cellular and mitochondrial iron homeostasis in vertebrates. Biochim Biophys Acta 2012; 1823:1459-67; PMID:22285816; http://dx.doi.org/10.1016/j.bbamcr.2012.01.003
2. Sheftel AD, Mason AB, Ponka P. The long history of iron in the Universe and in health and disease. Biochim Biophys Acta 2012; 1820:161-87; PMID:21856378; http://dx.doi.org/10.1016/j.bbagen.2011.08.002
3. Lill R, Hoffmann B, Molik S, Pierik AJ, Rietzschel N, Stehling O, Uzarska MA, Webert H, Wilbrecht C, Mühlenhoff U. The role of mitochondria in cellular iron-sulfur protein biogenesis and iron metabolism. Biochim Biophys Acta 2012; 1823:1491-508; PMID:22609301; http://dx.doi.org/10.1016/j.bbamcr.2012.05.009
4. Paradkar PN, Zumbrennen KB, Paw BH, Ward DM, Kaplan J. Regulation of mitochondrial iron import through differential turnover of mitoferrin 1 and mitoferrin 2. Mol Cell Biol 2009; 29:1007-16; PMID:19075006; http://dx.doi.org/10.1128/MCB.01685-08
5. Xu W, Barrientos T, Andrews NC. Iron and copper in mitochondrial diseases. Cell Metab 2013; 17:319-28; PMID:23473029; http://dx.doi.org/10.1016/j.cmet.2013.02.004
6. Colombini M. VDAC structure, selectivity, and dynamics. Biochim Biophys Acta 2012; 1818:1457-65; PMID:22240010; http://dx.doi.org/10.1016/j.bbamem.2011.12.026
7. Fleming MD, Romano MA, Su MA, Garrick LM, Garrick MD, Andrews NC. Nramp2 is mutated in the anemic Belgrade (b) rat: evidence of a role for Nramp2 in endosomal iron transport. Proc Natl Acad Sci U S A 1998; 95:1148-53; PMID:9448300; http://dx.doi.org/10.1073/pnas.95.3.1148
8. Zhang AS, Enns CA. Molecular mechanisms of normal iron homeostasis. Hematology Am Soc Hematol Educ Program 2009: 207-14; PMID:20008200; http://dx.doi.org/10.1182/asheducation-2009.1.207
9. Wolff NA, Ghio AJ, Garrick LM, Garrick MD, Zhao L, Fenton RA, Thévenod F. Evidence for mitochondrial localization of divalent metal transporter 1 (DMT1). FASEB J 2014; 28:2134-45; PMID:24448823; http://dx.doi.org/10.1096/fj.13-240564
10. Bolte S, Cordelieres FP. A guided tour into subcellular colocalization analysis in light microscopy. J Microsc 2006; 224:213-32; PMID:17210054; http://dx.doi.org/10.1111/j.1365-2818.2006.01706.x
11. Woost PG, Orosz DE, Jin W, Frisa PS, Jacobberger JW, Douglas JG, Hopfer U. Immortalization and characterization of proximal tubule cells derived from kidneys of spontaneously hypertensive and normotensive rats. Kidney Int 1996; 50:125-34; PMID:8807581; http://dx.doi.org/10.1038/ki.1996.295
12. Abouhamed M, Gburek J, Liu W, Torchalski B, Wilhelm A, Wolff NA, Christensen EI, Thévenod F, Smith CP. Divalent metal transporter 1 in the kidney proximal tubule is expressed in late endosomeslysosomal membranes: implications for renal handling of protein-metal complexes. Am J Physiol Renal Physiol 2006; 290:F1525-F1533; PMID:16449358; http://dx.doi.org/10.1152/ajprenal.00359.2005
13. Porcelli AM, Ghelli A, Zanna C, Pinton P, Rizzuto R, Rugolo M. pH difference across the outer mitochondrial membrane measured with a green fluorescent protein mutant. Biochem Biophys Res Commun 2005; 326:799-804; PMID:15607740; http://dx.doi.org/10.1016/j.bbrc.2004.11.105
14. Richardson DR, Lane DJ, Becker EM, Huang ML, Whitnall M, Suryo RY, Sheftel AD, Ponka P. Mitochondrial iron trafficking and the integration of iron metabolism between the mitochondrion and cytosol. Proc Natl Acad Sci U S A 2010; 107:10775-82; PMID:20495089; http://dx.doi.org/10.1073/pnas.0912925107
15. Sheftel AD, Richardson DR, Prchal J, Ponka P. Mitochondrial iron metabolism and sideroblastic anemia. Acta Haematol 2009; 122:120-33; PMID:19907149; http://dx.doi.org/10.1159/000243796
16. Pantopoulos K, Porwal SK, Tartakoff A, Devireddy L. Mechanisms of mammalian iron homeostasis. Biochemistry 2012; 51:5705-24; PMID:22703180; http://dx.doi.org/10.1021/bi300752r
17. Pagliarini DJ, Calvo SE, Chang B, Sheth SA, Vafai SB, Ong SE, Walford GA, Sugiana C, Boneh A, Chen WK, et al. A mitochondrial protein compendium elucidates complex I disease biology. Cell 2008; 134:112-23; PMID:18614015; http://dx.doi.org/10.1016/j.cell.2008.06.016
18. Nilsson R, Schultz IJ, Pierce EL, Soltis KA, Naranuntarat A, Ward DM, Baughman JM, Paradkar PN, Kingsley PD, Culotta VC, et al. Discovery of genes essential for heme biosynthesis through large-scale gene expression analysis. Cell Metab 2009; 10:119-30; PMID:19656490; http://dx.doi.org/10.1016/j.cmet.2009.06.012
19. Monné M, Palmieri F. Antiporters of the mitochondrial carrier family. Curr Top Membr 2014; 73:289-20; PMID:24745987; http://dx.doi.org/10.1016/B978-0-12-800223-0.00008-6
20. Gunshin H, Mackenzie B, Berger UV, Gunshin Y, Romero MF, Boron WF, Nussberger S, Gollan JL, Hediger MA. Cloning and characterization of a mammalian proton-coupled metal-ion transporter. Nature 1997; 388:482-8; PMID:9242408; http://dx.doi.org/10.1038/41343
21. Garrick MD, Kuo HC, Vargas F, Singleton S, Zhao L, Smith JJ, Paradkar P, Roth JA, Garrick LM. Comparison of mammalian cell lines expressing distinct isoforms of divalent metal transporter 1 in a tetracycline-regulated fashion. Biochem J 2006; 398:539-46; PMID:16737442; http://dx.doi.org/10.1042/BJ20051987
22. Mackenzie B, Ujwal ML, Chang MH, Romero MF, Hediger MA. Divalent metal-ion transporter DMT1 mediates both H^+ -coupled Fe2+ transport and uncoupled fluxes. Pflugers Arch 2006; 451:544-58; PMID:16091957; http://dx.doi.org/10.1007/s00424-005-1494-3
23. Trinder D, Oates PS, Thomas C, Sadleir J, Morgan EH. Localisation of divalent metal transporter 1 (DMT1) to the microvillus membrane of rat duodenal enterocytes in iron deficiency, but to hepatocytes in iron overload. Gut 2000; 46:270-6; PMID:10644324; http://dx.doi.org/10.1136/gut.46.2.270
24. Ke Y, Chen YY, Chang YZ, Duan XL, Ho KP, Jiang DH, Wang K, Qian ZM. Post-transcriptional expression of DMT1 in the heart of rat. J Cell Physiol 2003; 196:124-30; PMID:12767048; http://dx.doi.org/10.1002/jcp.10284
25. Petrat F, Weisheit D, Lensen M, de GH, Sustmann R, Rauen U. Selective determination of mitochondrial chelatable iron in viable cells with a new fluorescent sensor. Biochem J 2002; 362:137-47; PMID:11829750; http://dx.doi.org/10.1042/0264-6021:3620137
26. Petrat F, de GH, Rauen U. Subcellular distribution of chelatable iron: a laser scanning microscopic study in isolated hepatocytes and liver endothelial cells. Biochem J 2001; 356:61-9; PMID:11336636; http://dx.doi.org/10.1042/0264-6021:3560061
27. Drysdale J, Arosio P, Invernizzi R, Cazzola M, Volz A, Corsi B, Biasiotto G, Levi S. Mitochondrial ferritin: a new player in iron metabolism. Blood Cells Mol Dis 2002; 29:376-83; PMID:12547228; http://dx.doi.org/10.1006/bcmd.2002.0577
28. Hamza I, Dailey HA. One ring to rule them all: Trafficking of heme and heme synthesis intermediates in the metazoans. Biochim Biophys Acta 2012; 1823:1617-32; PMID:22575458; http://dx.doi.org/10.1016/j.bbamcr.2012.04.009
29. Ajioka RS, Phillips JD, Kushner JP. Biosynthesis of heme in mammals. Biochim Biophys Acta 2006; 1763:723-36; PMID:16839620; http://dx.doi.org/10.1016/j.bbamcr.2006.05.005
30. Mackenzie B, Takanaga H, Hubert N, Rolfs A, Hediger MA. Functional properties of multiple isoforms of human divalent metal-ion transporter 1 (DMT1). Biochem J 2007; 403:59-69; PMID:17109629; http://dx.doi.org/10.1042/BJ20061290
31. Illing AC, Shawki A, Cunningham CL, Mackenzie B. Substrate profile and metal-ion selectivity of human divalent metal-ion transporter-1. J Biol Chem 2012; 287:30485-96; PMID:22736759; http://dx.doi.org/10.1074/jbc.M112.364208
32. Flynn JM, Melov S. SOD2 in mitochondrial dysfunction and neurodegeneration. Free Radic Biol Med 2013; 62:4-12; PMID:23727323; http://dx.doi.org/10.1016/j.freeradbiomed.2013.05.027
33. Kawaguchi T, Noji S, Uda T, Nakashiman Y, Takeyasu A, Kawai Y, Takagi H, Tohyama M, Taniguchi N. A monoclonal antibody against COOH-terminal peptide of human liver manganese superoxide dismutase. J Biol Chem 1989; 264:5762-67; PMID:2647725
34. Aguirre JD, Culotta VC. Battles with iron: manganese in oxidative stress protection. J Biol Chem 2012; 287:13541-48; PMID:22247543; http://dx.doi.org/10.1074/jbc.R111.312181
35. Roth J, Ponzoni S, Aschner M. Manganese homeostasis and transport. Met Ions Life Sci 2013; 12:169-201; PMID:23595673; http://dx.doi.org/10.1007/978-94-007-5561-1_6
36. Portnoy ME, Liu XF, Culotta VC. Saccharomyces cerevisiae expresses three functionally distinct homologues of the nramp family of metal transporters. Mol Cell Biol 2000; 20:7893-902; PMID:11027260; http://dx.doi.org/10.1128/MCB.20.21.7893-7902.2000
37. Sickmann A, Reinders J, Wagner Y, Joppich C, Zahedi R, Meyer HE, Schonfisch B, Perschil I, Chacinska A, Guiard B, et al. The proteome of Saccharomyces cerevisiae mitochondria. Proc Natl Acad Sci U S A 2003; 100:13207-12; PMID:14576278; http://dx.doi.org/10.1073/pnas.2135385100
38. Avila DS, Puntel RL, Aschner M. Manganese in health and disease. Met Ions Life Sci 2013; 13:199-227; PMID:24470093; http://dx.doi.org/10.1007/978-94-007-7500-8_7
39. Salazar J, Mena N, Hunot S, Prigent A, Alvarez-Fischer D, Arredondo M, Duyckaerts C, Sazdovitch V, Zhao L, Garrick LM, et al. Divalent metal transporter 1 (DMT1) contributes to neurodegeneration in animal models of Parkinson's disease. Proc Natl Acad Sci U S A 2008; 105:18578-83; PMID:19011085; http://dx.doi.org/10.1073/pnas.0804373105
40. Tennant J, Stansfield M, Yamaji S, Srai SK, Sharp P. Effects of copper on the expression of metal transporters in human intestinal Caco-2 cells. FEBS Lett 2002; 527:239-44; PMID:12220667; http://dx.doi.org/10.1016/S0014-5793(02)03253-2
41. Arredondo M, Munoz P, Mura CV, Nunez MT. DMT1, a physiologically relevant apical Cu1+ transporter of intestinal cells. Am J Physiol Cell Physiol 2003; 284:C1525-C1530; PMID:12734107; http://dx.doi.org/10.1152/ajpcell.00480.2002
42. Jiang L, Garrick MD, Garrick LM, Zhao L, Collins JF. Divalent metal transporter 1 (Dmt1) mediates copper transport in the duodenum of iron-deficient rats and when overexpressed in iron-deprived HEK-293 cells. J Nutr 2013; 143:1927-33; PMID:24089420; http://dx.doi.org/10.3945/jn.113.181867
43. Arredondo M, Mendiburo MJ, Flores S, Singleton ST, Garrick MD. Mouse divalent metal transporter 1 is a

copper transporter in HEK293 cells. Biometals 2014; 27:115-23; PMID:24327293; http://dx.doi.org/10.1007/s10534-013-9691-6
44. Cobine PA, Ojeda LD, Rigby KM, Winge DR. Yeast contain a non-proteinaceous pool of copper in the mitochondrial matrix. J Biol Chem 2004; 279:14447-55; PMID:14729672; http://dx.doi.org/10.1074/jbc.M312693200
45. Cobine PA, Pierrel F, Bestwick ML, Winge DR. Mitochondrial matrix copper complex used in metallation of cytochrome oxidase and superoxide dismutase. J Biol Chem 2006; 281:36552-9; PMID:17008312; http://dx.doi.org/10.1074/jbc.M606839200
46. Cobine PA, Pierrel F, Winge DR. Copper trafficking to the mitochondrion and assembly of copper metalloenzymes. Biochim Biophys Acta 2006; 1763:759-72; PMID:16631971; http://dx.doi.org/10.1016/j.bbamcr.2006.03.002
47. Ferguson CJ, Wareing M, Ward DT, Green R, Smith CP, Riccardi D. Cellular localization of divalent metal transporter DMT-1 in rat kidney. Am J Physiol Renal Physiol 2001; 280:F803-14; PMID:11292622
48. Kuo HC, Smith JJ, Lis A, Zhao L, Gonsiorek EA, Zhou X, Higgins DM, Roth JA, Garrick MD, Garrick LM. Computer-identified nuclear localization signal in exon 1A of the transporter DMT1 is essentially ineffective in nuclear targeting. J Neurosci Res 2004; 76:497-511; PMID:15114622; http://dx.doi.org/10.1002/jnr.20112
49. Ott M, Robertson JD, Gogvadze V, Zhivotovsky B, Orrenius S. Cytochrome c release from mitochondria proceeds by a two-step process. Proc Natl Acad Sci U S A 2002; 99:1259-63; PMID:11818574; http://dx.doi.org/10.1073/pnas.241655498
50. Wieckowski MR, Giorgi C, Lebiedzinska M, Duszynski J, Pinton P. Isolation of mitochondria-associated membranes and mitochondria from animal tissues and cells. Nat Protoc 2009; 4:1582-90; PMID:19816421; http://dx.doi.org/10.1038/nprot.2009.151
51. Wolff NA, Lee WK, Abouhamed M, Thévenod F. Role of ARF6 in internalization of metal-binding proteins, metallothionein and transferrin, and cadmium-metallothionein toxicity in kidney proximal tubule cells. Toxicol Appl Pharmacol 2008; 230:78-85; PMID:18353411; http://dx.doi.org/10.1016/j.taap.2008.02.008
52. Wolff NA, Lee WK, Thévenod F. Role of Arf1 in endosomal trafficking of protein-metal complexes and cadmium-metallothionein-1 toxicity in kidney proximal tubule cells. Toxicol Lett 2011; 203:210-18; PMID:21421027; http://dx.doi.org/10.1016/j.toxlet.2011.03.014
53. Singh H, Lu R, Rodriguez PF, Wu Y, Bopassa JC, Stefani E, Toro L. Visualization and quantification of cardiac mitochondrial protein clusters with STED microscopy. Mitochondrion 2012; 12:230-6; PMID:21982778; http://dx.doi.org/10.1016/j.mito.2011.09.004